J. Am. Chem. Soc. **1996,** *118,* 421−428

Theoretical Study of the Reaction of Acetylene with B_4H_8. A Proposed Mechanism of Carborane Formation. 2

Michael L. McKee

Contribution from the Department of Chemistry, Auburn University, Auburn, Alabama 36849

Received May 15, 1995[⊗]

Abstract: A uniform computational level ([MP4/6-311+G(d,p)]//MP2/6-31G(d)+ZPC) is used to evaluate 18 intermediates and 12 transition states in the study of the mechanism of carborane formation, beginning with the elimination of H_2 from B_4H_{10} and ending with the formation of 1,2-$C_2B_4H_6$. The calculated activation barrier (33.0 kcal/mol) for the first step ($B_4H_{10} \rightarrow B_4H_8 + H_2$) is higher than experiment (23.7 kcal/mol) but in agreement with higher-level theory (CBS-Q, 34.4 kcal/mol). The first stable intermediate is a $-CH{=}CH-$ bridged B_4H_8 species, which is structurally similar to the known $-CH_2-CH_2-$ bridged B_4H_8 structure. The hydroboration pathway for insertion of C_2H_2 into a BH bond of B_4H_8 has a slightly lower activation barrier than the addition barrier of C_2H_2 to B_4H_8 (10.1 versus 13.1 kcal/mol, respectively). The hydroboration reaction leads, in a series of steps, to 2,5-μ-CH_2-1-CB_4H_7, a known product in the reaction of methylacetylene and B_4H_{10}.

Introduction

The reaction of acetylene with a boron hydride produces a number of different products depending on the reaction conditions.[1−7] With moderate heating (25−50 °C), the reaction of C_2H_2 with B_4H_{10} produces hydroboration products (alkylboranes) or *nido*-carboranes (e.g. CB_5H_9, $C_2B_4H_8$, $C_3B_3H_7$).[6] With more vigorous conditions, such as ac discharge, the reaction of C_2H_2 with B_2H_6 or B_5H_9 produces more compact structures, such as *closo*-carboranes, although in very small yields.[1,8,9]

In a series of papers, Grimes and co-workers investigated the reaction of B_4H_{10} and C_2H_2.[3−6] At 25−50 °C, they reported the major products as 2-CH_3-2,3,4-$C_3B_3H_6$ (**P1**), 2,3-$(CH_3)_2$-2,3,4-$C_3B_3H_5$ (**P2**), and 2,4-$(CH_3)_2$-2,3,4-$C_3B_3H_5$ (**P3**) with smaller yields of various non-methylated and other methylated *nido* cages, including 1,2-$C_2B_3H_7$, 2,3-$C_2B_4H_8$, 2,3,4-$C_3B_3H_7$, and 4-CH_3-4-CB_5H_8. From a study of the reactions of C_2D_2 with B_4H_{10}, Franz and Grimes[6] made three observations for the major products: (1) there was no detectable H−D scrambling on carbon at a cage vertex; (2) there was partial H−D substitution on methyl groups; (3) there were both trideuterated and tetradeuterated species.

From a consideration of the reaction products, Grimes and co-workers[6] put forward a mechanism (eqs 1a−h).

$$B_4H_{10} \rightarrow B_4H_8 + H_2 \tag{1a}$$

$$B_4H_8 + C_2H_2 \rightarrow C_2B_4H_{10} \tag{1b}$$

$$C_2B_4H_{10} \rightarrow C_2B_3H_7 + BH_3 \tag{1c}$$

$$C_2B_4H_{10} + C_2H_2 \rightarrow C_4B_4H_{12} \tag{1d}$$

$$C_4B_4H_{12} \rightarrow 2\text{-}CH_3\text{-}C_3B_3H_6 + BH_3 \tag{1e}$$

$$C_4B_4H_{12} + C_2H_2 \rightarrow C_6B_4H_{14} \tag{1f}$$

$$C_6B_4H_{14} \rightarrow 2,3\text{- and }2,4\text{-}(CH_3)_2\text{-}C_3B_3H_5 + CBH_3 \tag{1g}$$

$$C_6B_4H_{12} + C_2H_2 \rightarrow [C_2BH_4]_x \tag{1h}$$

Very recently Fox and Greatrex[10] have shown that several of the reactions products (**P2** and **P3**), originally believed[6] to be alkyl derivatives of $C_3B_3H_7$ based on ^{11}B NMR data available at that time, are in fact $C_2B_4H_8$ derivatives; this leaves **P1** as the only authentic $C_3B_3H_7$ derivative currently known.

The reaction has been determined to be first order in B_4H_{10} and zeroth order in C_2H_2. The activation energy (23.7 kcal/mol) and A factor (6.0×10^{11}) are similar to values found for other gas-phase reactions of B_4H_{10} for which the rate-determining step is assumed to be $B_4H_{10} \rightarrow B_4H_8 + H_2$ (eq 1a).[11] While the reactive intermediate B_4H_8 has not been isolated, mass spectra of B_4H_{10} and B_4H_8CO support its viability as an intermediate.[12]

It has been suggested that the diminished rate of reaction of pure B_4H_{10} compared to $B_4H_{10} + C_2H_2$ may be due to a rapid exchange between B_4H_{10} and B_4H_8/H_2 (k_1, eq 2).[6] If it is

$$B_4H_{10} \overset{k_1}{\rightleftarrows} B_4H_8 + H_2 \tag{2}$$

$$B_4H_{10} \xrightarrow{k_2} B_3H_7 + BH_3 \tag{3}$$

$$k_1 > k_2$$

assumed that the decomposition of pure B_4H_{10} is controlled by

---

[⊗] Abstract published in *Advance ACS Abstracts,* December 15, 1995.

(1) For an excellent review see: Williams, R. E. Early Carboranes and Their Structural Legacy. In *Advances in Organometallic Chemistry*; Stone, F. G. A., West, R., Eds.; Academic Press: New York, 1994, Vol 36; pp 1−55.

(2) Grimes, R. N. *J. Am. Chem. Soc.* **1966**, *88*, 1895.

(3) Grimes, R. N.; Bramlett, C. L. *J. Am. Chem. Soc.* **1967**, *89*, 2557.

(4) (a) Grimes, R. N.; Bramlett, C. L.; Vance, R. L. *Inorg. Chem.* **1968**, *7*, 1066. (b) Grimes, R. N.; Bramlett, C. L.; Vance, R. L. *Inorg. Chem.* **1969**, *8*, 55. (c) Bramlett, C. L.; Grimes, R. N. *J. Am. Chem. Soc.* **1966**, *88*, 4269.

(5) (a) Franz, D. A.; Grimes, R. N. *J. Am. Chem. Soc.* **1970**, *92*, 1438. (b) Franz, D. A.; Miller, V. R.; Grimes, R. N. *J. Am. Chem. Soc.* **1972**, *94*, 412.

(6) Franz, D. A.; Grimes, R. N. *J. Am. Chem. Soc.* **1971**, *93*, 387.

(7) Grimes, R. N. *Carboranes*; Academic Press: New York, 1970; pp 23−31.

(8) Shapiro, I.; Keilin, B.; Good, C. D.; Williams, R. E. *J. Am. Chem. Soc.* **1963**, *85*, 3167.

(9) Linder, H. H.; Onak, T. *J. Am. Chem. Soc.* **1966**, *88*, 1886.

(10) Fox, M. A.; Greatrex, R. *J. Chem. Soc., Chem. Commun.* **1995**, 667.

(11) (a) Greenwood, N. N. In *Electron Deficient Boron and Carbon Clusters*; Olah, G. A., Wade, K., Williams, R. E., Eds., Wiley: New York, 1991; pp 165−181. (b) Greatrex, R.; Greenwood, N. N.; Potter, C. D. *J. Chem. Soc., Dalton Trans.* **1984**, 2435. (c) Greatrex, R.; Greenwood, N. N.; Potter, C. D. *J. Chem. Soc., Dalton Trans.* **1986**, 81.

0002-7863/96/1518-0421$12.00/0

k_2 (eq 3), then in the presence of C_2H_2, B_4H_8 will react to form addition products and increase the rate of disappearance of B_4H_{10}. Support for rapid exchange comes from the observation of exchange between D_2 and B_4H_{10} and the synthesis of $B_4H_8D_2$ from B_4H_8CO and D_2.[13]

When methylacetylene (eq 4a) and dimethylacetylene (eq 5a) add to B_4H_{10}, the major volatile products are monomethyl- and dimethyl-substituted $C_2B_4H_8$, respectively.[4a] If the reaction of methyl- (eq 4b) or dimethylacetylene (eq 5b) with B_4H_{10} is quenched in a hot−cold reactor, a very different product is obtained.[14] The identity of this product was a mystery[15] until its recent elucidation[14] by the ab initio/IGLO/NMR structural determination method.[16] The structure has a B_5H_9 framework with an apical $CH_3{-}C$ group and either a bridging CH_2 (eq 4b) or a bridging $CH(CH_3)$ (eq 5b).

$$B_4H_{10} + CH_3C{\equiv}CH \rightarrow 2\text{-}CH_3\text{-}2,3\text{-}C_2B_4H_7 + H_2 \quad (4a)$$

$$B_4H_{10} + CH_3C{\equiv}CH \rightarrow 1\text{-}CH_3\text{-}2,5\text{-}\mu\text{-}CH_2\text{-}1\text{-}CB_4H_7 + H_2 \quad (4b)$$

$$B_4H_{10} + CH_3C{\equiv}CCH_3 \rightarrow 2,3\text{-}(CH_3)_2\text{-}2,3\text{-}C_2B_4H_6 + H_2 \quad (5a)$$

$$B_4H_{10} + CH_3C{\equiv}CCH_3 \rightarrow 1\text{-}CH_3\text{-}2,5\text{-}\mu\text{-}CH(CH_3)\text{-}1\text{-}CB_4H_7 + H_2 \quad (5b)$$

In the reaction of ethylene with B_4H_{10}, a structure with a B_4H_8 unit bridged by a $-CH_2CH_2-$ linkage is isolated (eq 6).[17] Franz and Grimes[6] speculated in the last line of their seminal manuscript on carborane formation that a similar compound (eq 7) might be isolated at low temperature from the reaction of B_4H_{10} with HC≡CH in a hot−cold reactor.

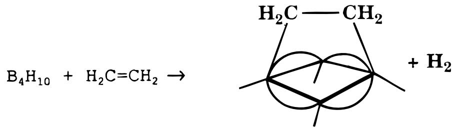

(6)

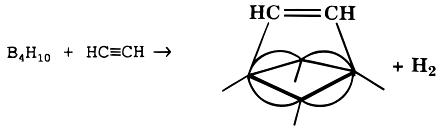

(7)

The only computational study dealing with the formation of carboranes from the addition of C_2H_2 to B_4H_{10} comes from a MNDO study by DeKock et al.[18] Although a mechanism was not presented, the authors suggested that a −HC═CH− bridged B_4H_8 species (eq 7) was on the reaction path. The driving force for the reaction (leading to 1,2-$C_2B_4H_6$) was suggested[18] to be due to the increase in boron−carbon bonding.

Method

All geometries were optimized at the MP2/6-31G(d) level.[19,20] Vibrational frequencies were calculated at that level to determine the nature of the potential-energy surface and to make zero-point corrections (frequencies weighted by a 0.95 factor). Single-point calculations were made at the MP4/6-31G(d) and MP2/6-311+G(d,p) levels and combined[21] to estimate relative energies at the [MP4/6-311+G(d,p)] level, which, when zero-point corrections have been added, will constitute the "standard" level. All MP2 and MP4 calculations were made with the "frozen-core" approximation.

Heat capacities and entropy corrections were made using unscaled frequencies and standard statistical procedures[22] to determine relative enthalpies and free energies at 298 K. Free energies at 500 K were estimated from eq 8.

$$\Delta G(500\text{K}) \approx \Delta H(298\text{K}) - 500\Delta S(298\text{K}) \qquad (8)$$

Molecular plots of all structures are given in Figure 1. A table of total energies (hartrees) and zero-point energies (kcal/mol) as well as **Z**-matrices of all species are provided as supporting information.

A boldface notation system is used for the species in the figures, tables, and text to aid in identification. For example, the bold notation **TS5/7** refers to the transition state between structures **5** and **7**, while the notation **TS2/1c+H$_2$** refers to the transition state for loss of H_2 from **2** to form **1c**. Relative energies (kcal/mol) are presented in Table 1 with respect to the top entry in each section of structures. In Table 2, enthalpies at 298 K and free energies at 298 and 500 K are tabulated relative to $B_4H_{10} + C_2H_2$ which is given a value of zero. A potential-energy diagram of enthalpies at 298 K is given in Figure 2 for the reaction path from B_4H_{10} (**2**) + C_2H_2 to the products 1,2-$C_2B_4H_6$ (**8**) + $3H_2$ and in Figure 3 for the hydroboration reaction path to **15**.

In the reaction of B_4H_{10} with C_2H_2, two main branches are considered. The first branch, beginning with the elimination of BH_3 from B_4H_{10} (eq 3), has already been calculated (Part 1);[23] the second branch, beginning with the elimination of H_2 from B_4H_{10} (eq 2), is the subject of the current investigation (Part 2). Since the computational levels of Part 1 and Part 2 are identical, the fate of reactive intermediates encountered in Part 2 can be inferred if they have previously been studied in Part 1. The current study has been limited to unimolecular reactions (except for the initial addition of C_2H_2 to B_4H_8), and to reactions which maintain a carbon−carbon bond.

Results and Discussion

Three structures were considered for isolated B_4H_8: quadruple-bridged with C_{2v} symmetry (**1a**), double-bridged with C_s symmetry (**1b**), and triple-bridged with C_1 symmetry (**1c**). While only the triple-bridged species (**1c**) is a minimum on the MP2/6-31G(d) surface, all three structures are within 3.0 kcal/

---

(12) (a) Baylis, A. B.; Pressley, G. A.; Gordon, M. E.; Stafford, F. E. *J. Am. Chem. Soc.* **1966**, *88*, 929. (b) Hollins, R. E.; Stafford, F. E. *Inorg. Chem.* **1970**, *9*, 877.

(13) (a) Todd, J. E.; Koski, W. S. *J. Am. Chem. Soc.* **1959**, *81*, 2319. (b) Norman, A. D.; Schaeffer, R. *J. Am. Chem. Soc.* **1966**, *88*, 1143.

(14) Fox, M. A.; Greatrex, R.; Hofmann, M.; Schleyer, P. v. R. *Angew. Chem., Int. Ed. Engl.* **1994**, *33*, 2298.

(15) (a) Greatrex, R.; Greenwood, N. N.; Kirk, M. *J. Chem. Soc., Chem. Commun.* **1991**, 1510. (b) Fox, M. A.; Greatrex, R.; Greenwood, N. N.; Kirk, M. *Polyhedron* **1993**, *12*, 1849.

(16) Onak, T.; Tran, D.; Tseng, J.; Diaz, M.; Arias, J.; Herrera, S. *J. Am. Chem. Soc.* **1993**, *115*, 9210 and references therein.

(17) (a) Hnyk, D.; Brain, P. T.; Rankin, D. W. H.; Robertson, H. E.; Greatrex, R.; Greenwood, N. N.; Kirk, M.; Bühl, M.; Schleyer, P. v. R. *Inorg. Chem.* **1994**, *33*, 2572. (b) Harrison, B. C.; Solomon, I. J.; Hites, R. D.; Klein, M. *J. Inorg. Nucl. Chem.* **1960**, *14*, 195. (c) For a methyl-substituted derivative see: Brain, P. T.; Bühl, M.; Fox, M. A.; Greatrex, R.; Leuschner, E.; Picton, M. J.; Rankin, D. W. H.; Robertson, H. E. *Inorg. Chem.* **1995**, *34*, 2841.

(18) DeKock, R. L.; Fehlner, T. P.; Housecroft, C. E.; Lubben, T. V.; Wade, K. *Inorg. Chem.* **1982**, *21*, 25.

(19) Frisch, M. J.; Trucks, G. W.; Schlegel, H. B.; Gill, P. M. W.; Johnson, B. G.; Wong, M. W.; Foresman, J. B.; Robb, M. A.; Head-Gordon, M.; Replogle, E. S.; Gomperts, R.; Andres, J. L.; Raghavachari, K.; Binkley, J. S.; Gonzalez, C.; Martin, R. L.; Fox, D. J.; Defrees, D. J.; Baker, J.; Stewart, J. J. P.; Pople, J. A. Gaussian92/DFT (Rev. G.2), Gaussian, Inc.: Pittsburgh, PA, 1993.

(20) Frisch, M. J.; Trucks, G. W.; Schlegel, H. B.; Gill, P. M. W.; Johnson, B. G.; Robb, M. A.; Cheeseman, J. R.; Keith, T.; Petersson, G. A.; Montgomery, J. A.; Raghavachari, K.; Al-Laham, M. A.; Zakrzewski, V. G.; Ortiz, J. V.; Foresman, J. B.; Cioslowski, J.; Stefanov, B. B.; Nanyakkara, A.; Challacombe, M.; Peng, C. Y.; Ayala, P. Y.; Chen, W.; Wong, M. W.; Andres, J. L.; Replogle, E. S.; Gomperts, R.; Martin, R. L.; Fox, D. J.; Binkley, J. S.; Defrees, D. J.; Baker, J.; Stewart, J. P.; Head-Gordon, M.; Gonzalez, C.; Pople, J. A. *Gaussian94* (Rev. B.1), Gaussian, Inc.: Pittsburgh, PA, 1995.

(21) (a) McKee, M. L.; Lipscomb, W. N. *J. Am. Chem. Soc.* **1981**, *103*, 4673. (b) Nobes, R. H.; Bouma, W. J.; Radom, L. *Chem. Phys. Lett.* **1982**, *89*, 497. (c) McKee, M. L.; Lipscomb, W. N. *Inorg. Chem.* **1985**, *24*, 762.

(22) McQuarrie, D. A. *Statistical Thermodynamics*; Harper & Row: New York, 1973.

(23) Part 1: McKee, M. L. *J. Am. Chem. Soc.* **1995**, *117*, 8001.

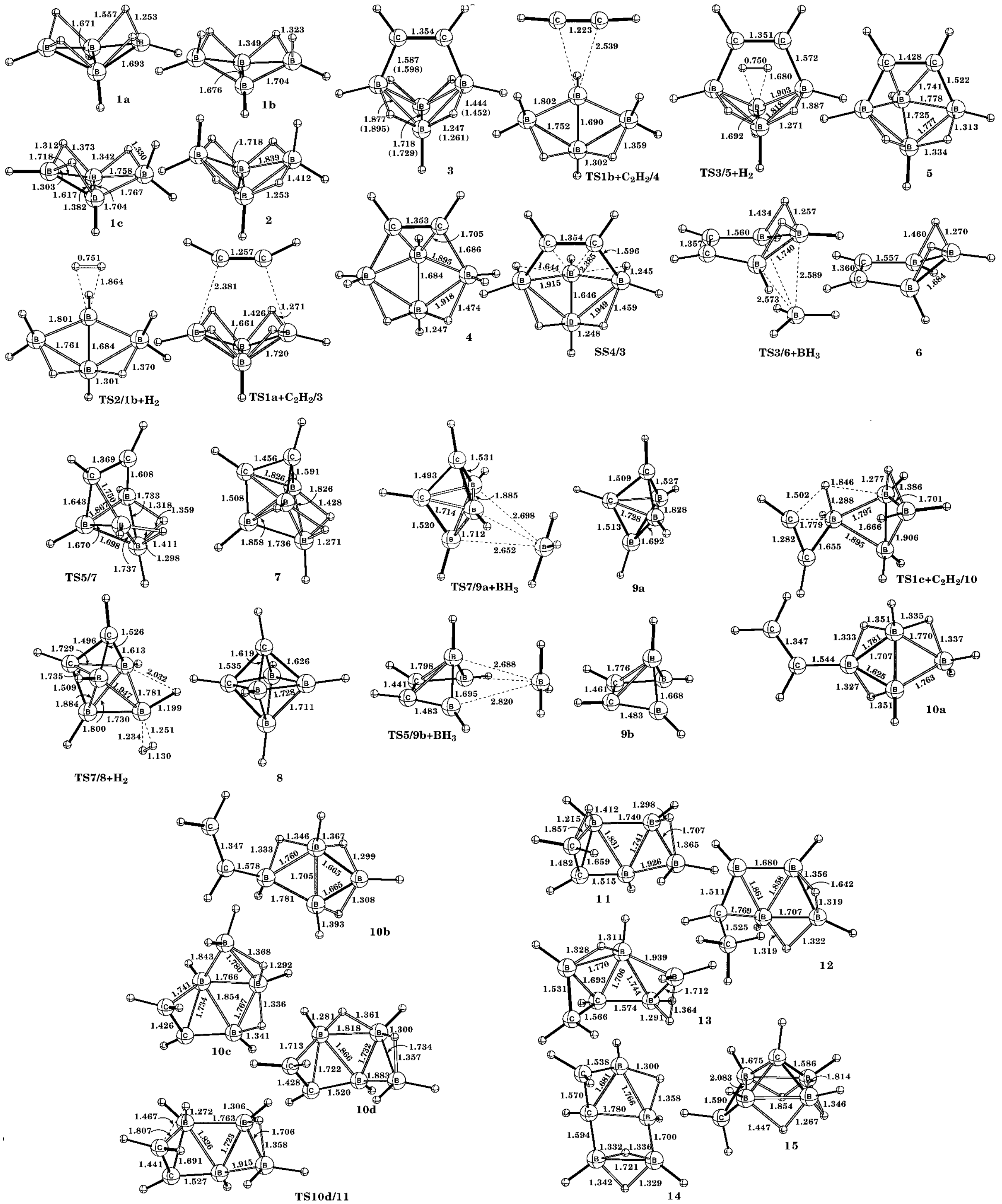

Figure 1. Selected geometric parameters of species optimized at the MP2/6-31G(d) level. The same boldface notations are used in the tables and text. The values in parentheses for **3** are experimental gas-phase values[17] for the related compound where $-CH_2-CH_2-$ replaces $-CH{=}CH-$.

mol at the standard level. Previous calculations on the three structures (**1a**−**c**) at a similar computational level ([MP4/6-311G(d,p)//MP2(FULL)/6-31G(d)]+6-31G(d)/ZPC) gave a range of 4.0 kcal/mol with **1c** lowest in energy.[24] The reaction energy of $B_4H_{10} \rightarrow B_4H_8$ (**1c**) + H_2 is 15.1 kcal/mol at the standard level compared to a previous result of 16.5 kcal/mol.[25] The free energy change between B_4H_{10} and B_4H_8 (**1c**) + H_2 is reduced to 7.3 kcal/mol at 298 K and only 1.2 kcal/mol at 500 K (Table 2). Such a small free energy difference supports the proposed equilibrium in eq 2.[6]

The activation barrier for H_2 elimination from B_4H_{10} has an experimentally determined activation barrier about 9 kcal/mol lower than calculated (23.7 kcal/mol, exptl;[13] 33.0 kcal/mol,

---

(24) McKee, M. L. *J. Am. Chem. Soc.* **1990**, *112*, 6753.

Table 1. Relative Energies, Enthalpies, and Free Energies (kcal/mol) of Various Species

	relative energies[a]					thermodynamic values[d]	
	MP2/a	MP4/a	MP2/b	[MP4/b][b]	+ZPC[c]	Δ*H* (298 K)	Δ*G* (298 K)
B_4H_{10} (**2**)	0.0	0.0	0.0	0.0	0.0	0.0	0.0
TS2/1c+H_2	41.5	39.7	39.2	37.4	33.0	33.4	32.4
B_4H_8 (**1a**) + H_2	29.2	28.2	29.1	28.1	17.8	18.6	10.6
B_4H_8 (**1b**) + H_2	27.8	25.9	28.7	26.8	18.1	19.3	10.1
B_4H_8 (**1c**) + H_2	22.2	21.1	23.2	22.1	15.1	16.3	7.3
B_4H_8 (**1c**) + C_2H_2	0.0	0.0	0.0	0.0	0.0	0.0	0.0
TS1a+C_2H_2/3	19.6	24.2	16.4	21.0	23.0	21.6	34.8
$C_2B_4H_{10}$ (**3**)	−53.3	−51.7	−54.2	−52.6	−46.5	−47.6	−35.8
TS1b+C_2H_2/4	12.0	12.0	12.2	12.2	13.1	13.7	23.0
$C_2B_4H_{10}$ (**4**)	−29.5	−26.6	−26.9	−24.0	−20.6	−21.3	−9.8
SS4/3	2.8	2.9	−0.2	−0.1	2.2	1.1	12.8
TS3/5+H_2	−10.8	−8.5	−14.3	−12.0	−8.7	−9.9	2.6
$C_2B_4H_8$ (**5**) + H_2	−78.4	−73.2	−73.9	−68.7	−67.4	−67.8	−63.3
TS3/6+BH_3	−10.9	−11.5	−11.0	−11.6	−8.5	−9.5	2.3
$C_2B_3H_7$ (**6**) + BH_3	−18.0	−18.1	−15.4	−15.4	−14.8	−15.0	−14.5
TS1c+C_2H_2/10	6.6	9.2	6.0	8.6	10.1	9.7	20.0
$H_2C{=}CH{-}B_4H_7$ (**10a**)	−46.6	−46.7	−45.7	−45.8	−40.3	−40.8	−30.2
$H_2C{=}CH{-}B_4H_7$ (**10b**)	−41.2	−41.5	−40.3	−40.6	−35.4	−35.9	−25.5
$C_2B_4H_{10}$ (**10c**)	−62.7	−58.6	−60.2	−56.1	−48.9	−50.1	−37.8
$C_2B_4H_{10}$ (**10d**)	−60.3	−56.7	−57.8	−54.2	−47.3	−48.5	−36.2
TS10d/11	−47.4	−43.9	−46.7	−43.2	−37.7	−38.3	−25.8
$C_2B_4H_{10}$ (**11**)	−48.7	−45.8	−47.8	−44.9	−38.3	−39.4	−27.1
CH_3-CB_4H_7 (**12**)	−46.1	−44.8	−44.7	−43.6	−36.3	−37.1	−25.9
CH_3-CB_4H_7 (**12′**)	−49.2	−47.8	−47.9	−46.5	−39.7	−40.3	−29.2
$C_2B_4H_{10}$ (**13**)	−66.9	−63.5	−64.2	−60.8	−53.4	−54.7	−42.7
$C_2B_4H_{10}$ (**14**)	−50.6	−48.0	−50.3	−47.7	−40.2	−41.5	−29.0
$C_2B_4H_{10}$ (**15**)	−85.0	−80.4	−83.4	−78.8	−71.7	−73.1	−60.2
$C_2B_4H_8$ (**5**)	0.0	0.0	0.0	0.0	0.0	0.0	0.0
TS5/7	54.5	52.1	52.1	49.7	47.2	47.3	47.1
$C_2B_4H_8$ (**7**)	35.5	36.1	33.6	34.2	32.5	32.7	32.4
TS7/8+H_2	79.6	80.1	74.4	74.9	69.1	69.9	68.4
1,2-$C_2B_4H_6$ (**8**) + H_2	12.5	15.1	13.4	16.0	8.6	10.1	1.5
TS7/9a+BH_3	72.9	71.9	72.5	71.5	66.2	67.0	65.4
TS5/9b+BH_3	90.3	86.6	89.2	85.5	80.2	81.2	79.0
1,2-$C_2B_3H_5$ (**9a**) + BH_3	75.7	74.8	75.9	75.0	67.6	69.2	56.7
$C_2B_3H_5$ (**9b**) + BH_3	92.2	89.0	91.6	88.4	81.0	82.9	69.8

[a] Basis set "a" is 6-31G(d). Basis set "b" is 6-311+G(d,p). [b] Values computed with additivity approximation. Δ*E*[MP4/b] = Δ*E*(MP4/a) + Δ*E*(MP2/b) − Δ*E*(MP2/a). [c] Zero-point correction made by weighting zero-point energies by a 0.95 factor. [d] Thermodynamic corrections have been computed with MP2/6-31G(d) vibrational frequencies.

calc). An earlier report of an activation barrier for H_2 elimination of 26.8 kcal/mol was in error.[25] The correct "best" value should have been 34.7 kcal/mol, in good agreement with the present value. The alternative mode of decomposition ($B_4H_{10} \rightarrow B_3H_7 + BH_3$) has an activation barrier of 37.6 kcal/mol (i.e. 4.6 kcal/mol higher than H_2 elimination).

Since there is disagreement between experiment and theory, a higher-level method was used to calculate the reaction and transition state to determine the activation barrier of the reaction $B_4H_{10} \rightarrow B_4H_8 + H_2$. Using CBS-Q (complete basis set method), which has been shown to provide better accuracy than G2,[26] the activation barrier is calculated to be 34.4 kcal/mol, in good agreement with the standard value in this paper of 33.0 kcal/mol. The reason for the disagreement between experiment and theory is not clear.

In the reaction of acetylene, the first assumed step is the elimination of H_2 from B_4H_{10} (eq 2). For the second step, addition of C_2H_2 to B_4H_8, two transition states were calculated. The first transition state, **TS1a+C_2H_2/3**, involves the symmetric addition of C_2H_2 to **1a**, the quadruply-bridged B_4H_8. It should be emphasized that the reactant is actually **1c** (not **1a**) because only **1c** is a energy minimum and that **TS1a+C_2H_2/3** is a transition state (one imaginary frequency). However, the B_4H_8 moiety in the transition state **TS1a+C_2H_2/3** strongly resembles **1a**. The forming C−B bonds are 2.381 Å in the transition state and the activation barrier is 23.0 kcal/mol. The product of C_2H_2 addition is **3**, a B_4H_8 unit bridged by a $-CH{=}CH-$ linkage, which is 46.5 kcal/mol lower in energy than B_4H_8 (**1c**) plus C_2H_2. The gas-phase structure has been determined (electron diffraction) for a very similar product ("basket with a handle"), obtained from the reaction of C_2H_4 with B_4H_{10}. Even though the "handle" is $-CH{=}CH-$ rather than $-CH_2{-}CH_2-$, the MP2/6-31G(d) calculated B−B and C−B distances of **3** are within 0.02 Å of the GED structure for the related compound.[17]

TS1a+C_2H_2/3 is not the lowest-energy transition state for addition of C_2H_2 to B_4H_8. Another transition state (with an activation barrier of 13.1 kcal/mol) exists, **TS1b+C_2H_2/4**, which resembles the addition of C_2H_2 to **1b**, the double-bridged B_4H_8 structure. In this transition state, both carbons of acetylene interact with a single boron rather than with different borons as in **TS1a+C_2H_2/3**. The product is an *arachno* pentagonal bipyramid (**4**), 20.6 kcal/mol more stable than B_4H_8 (**1c**) plus C_2H_2.

---

(25) An error has been discovered in Table III of ref 24 for the reaction $B_4H_{10} \rightarrow B_4H_8 + H_2$ at the MP2/6-311G(d,p) level. The reported barrier (reaction energy) at that level, 31.3 (8.6) kcal/mol, is incorrect. The correct barrier (reaction energy), computed from the absolute energies in Table II,[24] is 39.2 (16.5) kcal/mol. As a consequence, the two pathways for unimolecular decomposition of B_4H_{10} (to B_3H_7 plus BH_3 and to B_4H_8 plus H_2) are much closer together than previously reported.[24]

(26) Montgomery, J. A.; Ochterski, J. W.; Petersson, G. A. *J. Chem. Phys.* **1994**, *101*, 5900.

(27) Bühl, M.; Schleyer, P. v. R. *J. Am. Chem. Soc.* **1992**, *114*, 477.

Table 2. Enthalpies and Free Energies (kcal/mol) Relative to B_4H_{10} Plus C_2H_2

	relative thermodynamic values		
	Δ*H* (298 K)	Δ*G* (298 K)	Δ*G* (500 K)
B_4H_{10} (**2**) + C_2H_2	0.0	0.0	0.0
TS2/1c+H₂, C_2H_2	33.4	32.4	31.6
B_4H_8 (**1a**) + H_2, C_2H_2	18.6	10.6	5.1
B_4H_8 (**1b**) + H_2, C_2H_2	19.3	10.1	3.9
B_4H_8 (**1c**) + H_2, C_2H_2	16.3	7.3	1.2
TS1a+C₂H₂/3, H_2	37.9	42.1	45.0
$C_2B_4H_{10}$ (**3**) + H_2	−31.3	−28.5	−26.6
TS1b+C₂H₂/4, H_2	30.0	30.3	30.5
$C_2B_4H_{10}$ (**4**) + H_2	−5.0	−2.5	−0.9
SS4/3 + H_2	17.4	20.1	21.9
TS3/5+H₂ + H_2	6.8	9.9	12.3
$C_2B_4H_8$ (**5**) + $2H_2$	−51.5	−56.0	−59.3
TS3/6+BH₃ + BH_3, H_2	6.8	9.6	11.5
$C_2B_3H_7$ (**6**) + BH_3, H_2	1.3	−7.2	−12.9
TS5/7 + H_2	−4.2	−8.9	−12.8
$C_2B_4H_8$ (**7**) + H_2	−18.8	−23.6	−27.1
TS7/8+H₂ + $2H_2$	18.4	12.4	8.0
1,2-$C_2B_4H_6$ (**8**) + $3H_2$	−41.4	−54.5	−63.6
TS7/9a+BH₃ + $2H_2$	15.5	9.4	5.1
TS5/9b+BH₃ + $2H_2$	29.7	23.0	18.2
1,2-$C_2B_3H_5$ (**9a**) + BH_3, $2H_2$	17.7	0.7	−11.1
$C_2B_3H_5$ (**9b**) + BH_3, $2H_2$	31.4	13.8	1.6
TS1c+C₂H₂/10 + H_2	26.0	27.3	28.2
$H_2C{=}CH\text{-}B_4H_7$ (**10a**) + H_2	−24.5	−22.9	−21.9
$H_2C{=}CH\text{-}B_4H_7$ (**10b**) + H_2	−19.6	−18.2	−17.3
$C_2B_4H_{10}$ (**10c**) + H_2	−33.8	−30.5	−28.3
$C_2B_4H_{10}$ (**10d**) + H_2	−32.2	−28.9	−26.6
TS10d/11 + H_2	−22.0	−18.5	−16.1
$C_2B_4H_{10}$ (**11**) + H_2	−23.1	−19.8	−17.6
$CH_3\text{-}CB_4H_7$ (**12**) + H_2	−20.8	−18.6	−16.6
$CH_3\text{-}CB_4H_7$ (**12′**) + H_2	−24.0	−21.9	−20.5
$C_2B_4H_{10}$ (**13**) + H_2	−38.4	−35.4	−32.6
$C_2B_4H_{10}$ (**14**) + H_2	−25.2	−21.7	−19.3
$C_2B_4H_{10}$ (**15**) + H_2	−56.8	−52.9	−50.3

A structure (**SS4/3**) was located for the interconversion of **4** to **3** which is 22.6 kcal/mol higher in energy than **4**. **SS4/3** is a stationary state of second order (two imaginary frequencies) which implies that the true transition state connecting **4** and **3** must have lower energy than **SS4/3** (i.e. the activation barrier **4** → **3** must be less than 22.6 kcal/mol). Besides the transition vector relating **4** and **3**, **SS4/3** has a second transition vector with motion toward a triple-bridged B_4H_8 moiety. Thus, it appears that **SS4/3** is affected by the same stabilizing influence which makes triple-bridged B_4H_8 (**1c**) more stable than double-bridged (**1b**). An estimate of the activation barrier **4** → **3** might be taken as **SS4/3** minus the **1c** − **1b** energy difference (4.0 kcal/mol), or about 19 kcal/mol. In any event, the lowest-energy pathway for forming **3** from B_4H_8 plus C_2H_2 is **TS1b+C₂H₂/4** → **4** → **SS4/3** → **3** rather than the direct pathway, **TS1a+C₂H₂/3** → **3**.

There are two unimolecular pathways for decomposition of **3**, elimination of H_2 to form $C_2B_4H_8$ (**5**) and elimination of BH_3 to form $C_2B_3H_7$ (**6**). The two pathways have nearly the same activation barriers. The first pathway (**TS3/5+H₂**) has a barrier of 37.8 kcal/mol, while the second pathway (**TS3/6+BH₃**) has a barrier of 38.0 kcal/mol.

The elimination of H_2 from $C_2B_4H_{10}$ (**3**) to form $C_2B_4H_8$ (**5**) occurs in two stages. From **3** to the transition state, **TS3/5+H₂**, two bridge hydrogens are converted into a hydrogen molecule with very little change to the remainder of the transition state. After the transition state, the C═C bond interacts with the now under-saturated boron center, forming two new C−B bonds and causing the C−C bond to lengthen from 1.351 Å in **TS3/5+H₂** to 1.428 Å in **5**. The carborane **5** is a well-known carborane whose structure and properties have been calculated and compared with experiment.[26] It has been observed in the low-temperature reactions of B_4H_{10} with C_2H_2 in both the C-methylated and unmethylated form.[6]

The transition state for the reaction **3** → **TS3/6+BH₃** → **6** + BH_3 is very late, as judged by the long B−B distances of the departing BH_3 unit (2.573, 2.589 Å). The reverse reaction (**6** + BH_3 → **TS3/6+BH₃** → **3**) corresponds to the conversion of two terminal B−H bonds of BH_3 to bridging interactions in **3**, which requires only a small activation barrier (5.5 kcal/mol). The free carborane $C_2B_3H_7$ (**6**) has not been observed, although complexes with transition metals have.[28]

closo-1,2-$C_2B_4H_6$ (**8**) can be formed from **5** by loss of molecular hydrogen. However, no direct reaction pathway for the transformation could be found. After much searching, an intermediate (**7**) was found with C_s symmetry which was 32.5 kcal/mol higher in energy than **5**. A "local bond rotation" (rotation of the C−C bond pair around an axis connecting the C−C bond midpoint and the center of the molecule)[29] connects the reactant (**5**) with the transition state (**TS5/7**) and product (**7**). The transition state (**TS5/7**) is late as evidenced by a large forward barrier (47.3 kcal/mol) and small reverse barrier (14.6 kcal/mol).

A bridge hydrogen and terminal hydrogen are eliminated as molecular hydrogen in the C_1-symmetry transition state (**TS7/8+H₂**). A more direct pathway of C_s symmetry, in which two bridge hydrogens are eliminated to form molecular hydrogen, is blocked by a HOMO/LUMO crossing.[30] As the bridge/terminal hydrogen pair is eliminated, the second bridge hydrogen is converted into a terminal hydrogen.

The $C_2B_4H_8$ intermediate (**7**) can also eliminate BH_3 with an activation barrier (**TS7/9a+BH₃**) slightly lower than that for eliminating H_2 via **TS7/8+H₂** (15.5 versus 18.4 kcal/mol, respectively). The product, 1,2-$C_2B_3H_5$ carborane (**9a**), was found in Part 1 to be separated from B_3H_7 + C_2H_2 by relatively higher barriers. The current transition state, **TS7/9a+BH₃**, provides a lower-energy pathway to **9a**.

$C_2B_4H_8$ (**5**) can also lose BH_3 to form a carborane **9b** via transition state **TS5/9b+BH₃**. Since **9b** was calculated in Part 1 to have a 1.0 kcal/mol activation barrier for formation of **9a**, both transition states, **TS7/9a+BH₃** and **TS5/9b+BH₃**, provide **9a** as the stable carborane.

If $C_2B_3H_5$ (**9a**/**9b**) and BH_3 are calculated separately and their energies added, the energies are 2.2 and 0.8 kcal/mol higher than **TS7/9a+BH₃** and **TS5/9b+BH₃**, respectively, which indicates that the first products of reaction are an association of **9a** and **9b** with BH_3. Since borane (BH_3) is known to form complexes with a variety of species (including H_2), an initial stabilizing association is not completely unexpected.

At 500 K, the most favorable products from B_4H_{10} and C_2H_2 are 1,2-$C_2B_4H_6$ (**8**) + $3H_2$ (63.6 kcal/mol lower in free energy, Table 2). In addition, all free energies of activation at 500 K are less than the initial free energy barrier for elimination of H_2 from B_4H_{10} (**TS2/1c+H₂**). Thus, under conditions of high local heating (e.g. ac discharge) reaction products which have a large increase in entropy are favored (Δ*S* for the reaction, $B_4H_{10} + C_2H_2 \rightarrow C_2B_4H_6 + 3H_2$, is predicted to be 44 eu).

---

(28) Many complexes of $C_2B_3H_7$ or $C_2B_3H_5^{2-}$ with different transition metals are known. The following are two examples. (a) Sneddon, L. G.; Beer, D. C.; Grimes, R. N. *J. Am. Chem. Soc.* **1973**, *95*, 6623. (b) Spencer, J. T.; Grimes, R. N. *Organometallics* **1987**, *6*, 323.

(29) McKee, M. L. *J. Am. Chem. Soc.* **1988**, *110*, 5317.

(30) (a) Gimarc, B. M.; Ott, J. J. *Inorg. Chem.* **1986**, *25*, 83. (b) Gimarc, B. M.; Ott, J. J. *Inorg. Chem.* **1986**, *25*, 2708. (c) Gimarc, B. M.; Ott, J. J. *J. Comput. Chem.* **1986**, *7*, 673.

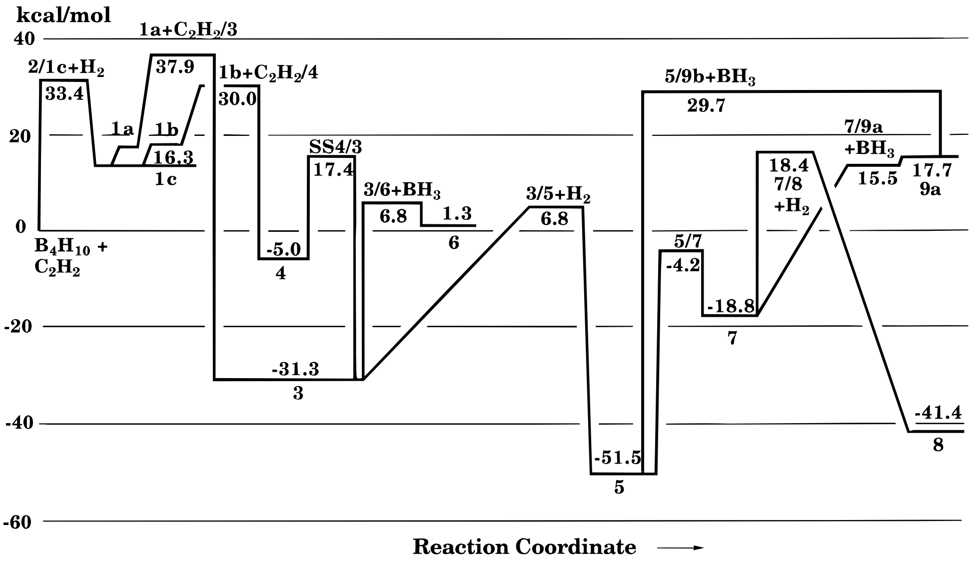

Figure 2. Plot of enthalpies (kcal/mol, 298 K) of minima and transition states relative to $B_4H_{10} + C_2H_2$ (see Table 2) leading to 1,2-$C_2B_4H_6$.

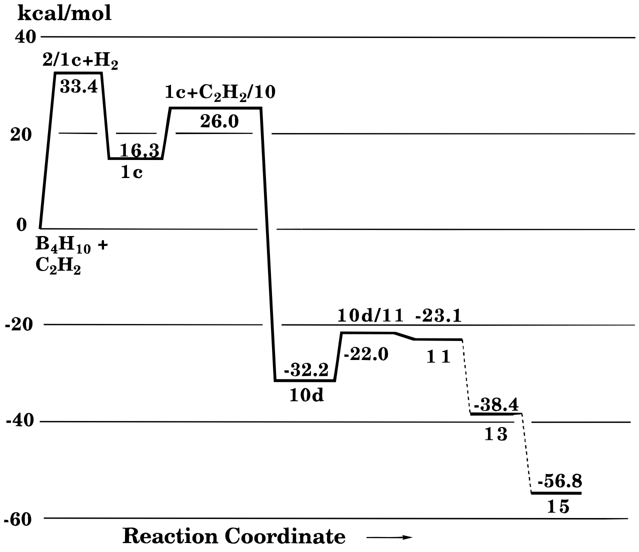

Figure 3. Plot of enthalpies (kcal/mol, 298 K) of minima and transition states relative to $B_4H_{10} + C_2H_2$ for the hydroboration branch of the reaction. The dotted lines connecting **11** → **13** and **13** → **15** signify that transition states have not been located between these pairs of species.

Hydroboration Pathway

Besides the addition of C_2H_2 to B_4H_8, the initial reaction step can be a hydroboration step, the transfer of boron to one end of acetylene and hydrogen to the other end (Figure 3). A transition state (**TS1c+C$_2$H$_2$/10**) was located for this process with an activation barrier of only 10.1 kcal/mol. The transferring hydrogen is 1.502 Å from carbon while still unsymmetrically bridged between two borons (1.288 and 1.846 Å) in the transition state. The extent of C−B formation is already significant in the transition state (1.655 Å).

There are five B−H terminal hydrogens in triple-bridged B_4H_8 (**1c**). Replacing any terminal hydrogen with a $-CH{=}CH_2$ group yields a possible hydroboration product. While only four species (**10a−d**) have been calculated, undoubtedly many more isomers and conformations exit. The four species considered have C_1 symmetry, are confirmed to be minima, and are within 13.5 kcal/mol of each other. The vinyl-substituted B_4H_8 structures **10a** and **10b** are 40.3 and 35.4 kcal/mol more stable than B_4H_8 (**1c**) + C_2H_2, respectively. In structures **10c** and **10d**, the vinyl group is allowed to interact with an adjacent boron center, which forms a bridging methylene center. In the case of $H_2C{=}HC{-}B_3H_6$, one of the possible isomers forms a bridging methylene center without activation.[23] It is probable that **10a−d** can all interconvert with small activation barriers which means that the product of hydroboration should be an equilibrium of **10c** and **10d** which are 48.9 and 47.3 kcal/mol lower than **1c** + C_2H_2, respectively. From **10d**, a transition state (**TS10d/11**) was located for the formation of an unusual carborane (**11**) with a bridging C−H$_b$−B. The activation barrier is 9.6 kcal/mol, but the product (**11**) is only 0.6 kcal/mol lower in energy than the transition state (**TS10d/11**). Breaking the C−H$_b$−B bond in **11** on the boron side results in the formation of a methyl-substituted *nido*-carborane CH_3-CB_4H_7 (**12**) which is 2.0 kcal/mol higher in energy than **11**. Although not calculated, a transition state must exist between **11** and **12** since **12** is a confirmed minimum. If the H/Me substituents on carbon are switched in **12**, another structure (**12′**, not shown in Figure 1) is calculated which is 3.4 kcal/mol lower in energy than **12**.

If the concentration of **12** (or **12′**) is sufficiently large, bimolecular reactions with C_2H_2 might give rise to methyl-substituted $C_2B_4H_8$ (eq 9). In the case of $B_3H_7 + C_2H_2$, a similar

$$CH_3\text{-}CB_4H_7\ (\mathbf{12}) + C_2H_2 \rightarrow CH_3\text{-}C_3B_4H_9 \rightarrow (CH_3)_2\text{-}C_2B_4H_6 \quad (9)$$

product, $CH_3{-}CB_3H_6$, was found[23] to be the global minimum on the $C_2B_3H_9$ potential energy surface. The reaction with C_2H_2 and elimination of H_2 (eq 10) gives methyl-substituted $C_3B_3H_7$

$$CH_3\text{-}CB_3H_6 + C_2H_2 \rightarrow CH_3\text{-}C_3B_3H_8 \rightarrow CH_3\text{-}C_3B_3H_6 + H_2 \quad (10)$$

which is one of the products observed in the low-temperature reaction of $B_4H_{10} + C_2H_2$.[6,10]

In the reaction of methylacetylene with B_4H_{10}, a $C_3B_4H_{14}$ product is formed, whose NMR spectra was known but whose structure long evaded researchers.[15] The structure finally

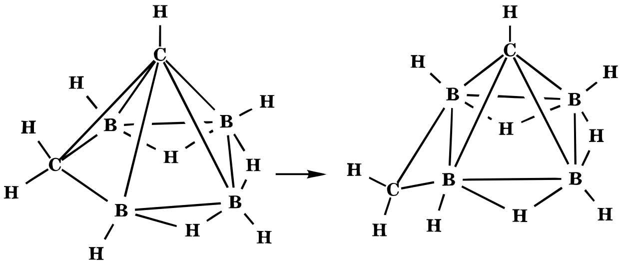

Figure 4. Possible pentagonal pyramidal structure of $C_2B_4H_{10}$. Optimization of this structure led without barrier to **15** via a diamond−square−diamond (DSD) mechanism.

succumbed[14] to the powerful ab initio/IGLO/NMR method developed by Schleyer and co-workers.[16] In this method, an exhaustive number of possible structural candidates is first optimized at a reliable level of theory (usually MP2/6-31G(d)) and then each is subjected to an IGLO calculation in order to determine the chemical shifts. Usually, exceptional agreement is found for one of the candidate structures and experiment, which secures its identification as the structure in solution. In the case of $C_3B_4H_{12}$, several factors misled researchers from considering what later turned out to be the correct structure. This structure is based on the B_5H_9 square-pyramidal structure with a methyl-substituted carbon in the apex position and a bridging CH_2 group. It is interesting to note that while the reaction of ethylacetylene with B_4H_{10} gave a similar structure, reaction of acetylene itself did not yield the characteristic NMR spectrum in solution.[14]

As stated in the Introduction, this study is limited to unimolecular reactions (except for the initial $B_4H_8 + C_2H_2$) and to structures which have direct carbon−carbon bonds. This restriction was eased in the case of the square-pyramidal structure (**15**) since that structure appears to be relevant to the reaction. Indeed, structure **15** is the global minimum on the $C_2B_4H_{10}$ potential energy surface, 71.7 kcal/mol more stable than B_4H_8 (**1c**) + C_2H_2. An attempt was made to find a path to **15** from **10c**/**10d**, but a transition state could not be located. If the $B_3H_7 + C_2H_2$ reaction can be used as a model,[23] a number of intermediates may exist with progressively longer C−C bonds. In other words, the double bond does not break in one step, rather the C═C double bond (**10a**/**10b**) is first converted into a C−C single bond (**10c**/**10d**) and then into a multicenter bond before finally breaking. Two structures, based on transition state candidates in the rearrangement of B_5H_9,[31] were located which might lie on the pathway for C−C bond breaking (**13** and **14**).

Both structures have longer C−C bonds than **10d** (1.566 Å, **13**; 1.570 Å, **14**; 1.428 Å, **10d**), indicating that **13** and/or **14** might be further along the reaction pathway toward **15**. Structure **13** (53.4 kcal/mol more stable than **1c** + C_2H_2) is a particularly attractive candidate since it is intermediate in stability between **10d** and **15**.

While transition states connecting **10d** → **13** → **15** could not be located, an optimization at the MP2/6-31G(d) level established that the pentagonal pyramid $C_2B_4H_{10}$ (Figure 4) is not a local minimum on the MP2/6-31G(d) potential energy surface; it rearranges instead to **15** via a diamond−square−diamond (DSD) mechanism.

Discussion

A series of reactions (eq 11a−h and 12a−d) illustrate the formation of known products in bold type):

$$B_4H_{10} \rightarrow B_3H_7 + BH_3 \tag{11a}$$

$$B_3H_7 + C_2H_2 \rightarrow C_2B_3H_9 \tag{11b}$$

$$C_2B_3H_9 \rightarrow \mathbf{C_2B_3H_7} + H_2 \tag{11c}$$

$$C_2B_3H_9 \rightarrow CH_3\text{-}CB_3H_6 \tag{11d}$$

$$B_4H_{10} \rightarrow B_4H_8 + H_2 \tag{11e}$$

$$B_4H_8 + C_2H_2 \rightarrow C_2B_4H_{10} \tag{11f}$$

$$C_2B_4H_{10} \rightarrow \mathbf{C_2B_4H_8} + H_2 \tag{11g}$$

$$C_2B_4H_{10} \rightarrow CH_3\text{-}CB_4H_7 \tag{11h}$$

$$CH_3\text{-}CB_3H_6 + C_2H_2 \rightarrow CH_3\text{-}C_3B_3H_8 \tag{12a}$$

$$CH_3\text{-}C_3B_3H_8 \rightarrow \mathbf{CH_3\text{-}C_3B_3H_6} + H_2 \tag{12b}$$

$$CH_3\text{-}CB_4H_7 + C_2H_2 \rightarrow \mathbf{(CH_3)_2\text{-}C_2B_4H_6} \tag{12c}$$

$$CH_3\text{-}CB_4H_7 + C_2H_2 \rightarrow \mathbf{C_2H_5\text{-}C_2B_4H_7} \tag{12d}$$

Reactions 11a−d have been calculated in Part 1,[23] reactions 11e−h have been calculated in Part 2, and reactions 12a−d are postulated to form observed products (boldface type) from reactive intermediates already calculated. The methyl-substituted *nido*-carboranes, CH_3-CB_3H_6 (eq 11d) and CH_3-CB_4H_7 (eq 11h), are relatively stable intermediates (especially CH_3-CB_3H_6) which can add another C_2H_2 to an unsaturated boron atom. Note that the reactions were carried out in a 10-fold excess of acetylene; this would increase the rate of reaction of eqs 12a,c,d.[4,6]

The reactivity of B_4H_8 and CB_3H_7[32] toward C_2H_2 (eqs 11f and 12a) should be similar since both have *nido* electron counts and have the same framework structure. Therefore, the product, $C_3B_3H_9$, might be expected to form via a similar mechanism (**2** + C_2H_2 → **4** → **3**) and to eliminate hydrogen to form $C_3B_3H_7$ (eq 12b) via a similar mechanism (eq 11g, **3** → **5** + H_2). Calculations at the standard level used in the present study confirm this analysis for the first step. The calculated activation barrier is 16.5 kcal/mol for the reaction C_2H_2 plus CB_3H_7 (compared to an activation barrier of 13.1 kcal/mol for **2** + C_2H_2 → **4**) to form $C_3B_3H_9$, which is predicted to be 24.1 kcal/mol exothermic (compared to 20.6 kcal/mol for the formation of **4**).

Conclusions

Carborane-forming reactions from acetylenes and boron hydrides have been known for over 40 years, yet their mechanism is poorly understood. A number of products are known and their concentrations are sensitive to the reaction conditions and ratio of acetylene to boron hydride. The present study is an initial attempt at considering various possible reactions. The reaction is divided into two major branches: the first branch, the reaction of C_2H_2 with B_3H_7, has been considered in Part 1, while the second branch, the reaction of C_2H_2 with

---

(31) McKee, M. L.; Lipscomb, W. N. *Inorg. Chem.* **1985**, *24*, 765.

(32) The calculated structure for CB_3H_7 agrees with the predicted structure by Williams. See ref 1, structure **58**.

B_4H_8, is considered here. For each branch, two general mechanisms are considered: first, the addition of C_2H_2 to the boron hydride (B_3H_7 or B_4H_8); and second, the insertion of C_2H_2 into a B−H bond of the boron hydride (B_3H_7 or B_4H_8).

The addition reactions, which lead to *nido*- and *closo*-carboranes, may be favored at high temperatures and long reaction times, since the products are generally more stable and are favored by entropy. The insertion reactions are favored at lower temperature and at short reaction times, because the initial insertion barrier is slightly lower in energy than the addition barrier.

Methylated products arise from the migration of a boron hydrogen to a methylene carbon in the insertion mechanism (forming CH_3-CB_3H_6 from $C_2H_2 + B_3H_7$ or CH_3-CB_4H_7 from $C_2H_2 + B_4H_8$) followed by subsequent addition of a second molecule of acetylene.

Acknowledgment. Computer time for this study was made available by the Alabama Supercomputer Network and the NSF-supported Pittsburgh Supercomputer Center. I thank Dr. Nico J. R. van Eikema Hommes for making Molecule available, which was used for drawing the structures in Figure 1. I would like to thank Professor R. N. Grimes for helpful correspondence.

Supporting Information Available: A table of total energies (hartrees) and zero-point energies (kcal/mol) and computer generated coordinates (**Z**-matrix) are available for all species optimized at the MP2/6-31G(d) level (26 pages). This material is contained in many libraries on microfiche, immediately follows this article in the microfilm version of the journal, can be ordered from the ACS, and can be downloaded from the Internet; see any current masthead page for ordering information and Internet access instructions.

JA951575C